Research Article Vol. 5, No. 5 / May 2018 / Optica 583

Temporal and polarization dependence of the nonlinear optical response of solvents

Peng Zhao,[1] Matthew Reichert,[1,2] Sepehr Benis,[1] David J. Hagan,[1,3] and Eric W. Van Stryland[1,3,*]

[1]CREOL, The College of Optics & Photonics, University of Central Florida, Orlando, Florida 32816, USA
[2]Department of Electrical Engineering, Princeton University, Princeton, New Jersey 08455, USA
[3]Department of Physics, University of Central Florida, Orlando, Florida 32816, USA
*Corresponding author: ewvs@creol.ucf.edu

Received 6 November 2017; revised 12 March 2018; accepted 10 April 2018 (Doc. ID 312933); published 8 May 2018

It has long been known that nonlinear refraction in solvents can depend on pulse width, and this along with experimental uncertainties has led to orders-of-magnitude disagreements in nonlinear refractive coefficients reported in the literature. To resolve this issue, we perform beam-deflection (BD) measurements of the rigorously defined nonlinear impulse response function for 24 commonly used solvents selected from various classes of molecules. Using this polarization-resolved BD, the bound-electronic and the three major nuclear contributions are separately measured by determining the magnitudes, symmetry, and temporal dynamics of each mechanism. This allows us to construct the response functions that we use to accurately establish self-consistent references for predicting and interpreting the outcomes of other experiments performed on these materials over the temporal range from 10 fs to 1 ns. The results also provide insight into relating solvent nonlinearities with their molecular structures and exploring the effects of the Lorentz–Lorenz local field. We find that nonconjugated molecules with small polarizability anisotropy exhibit negligible reorientational response, and hence the nonlinear refraction is almost independent of pulse width. Knowledge of the response functions also allows engineering the transient nonlinear refractive properties of solutions of organic dyes, for example, materials with effectively zero nonlinear refraction.

OCIS codes: (190.7110) Ultrafast nonlinear optics; (190.3270) Kerr effect; (190.5650) Raman effect; (160.4330) Nonlinear optical materials.

https://doi.org/10.1364/OPTICA.5.000583

1. INTRODUCTION

The nonlinear optical (NLO) response of organic solvents has long been studied in the visible and near-infrared spectral range, where they are nearly transparent. The knowledge of the absolute magnitudes and temporal dynamics of the NLO response is critical to interpreting the results performed on solutions of organic dyes, e.g., to separate the response of the solute. To quantify the nonlinear refraction (NLR), a single index, n_2, where $n(I) = n_0 + n_2 I$, with I the irradiance and n_0 the linear refractive index, is commonly used. However, in cases where the NLO response is not instantaneous, this single quantity is insufficient, which creates problems in comparing literature values [1,2]. For example, one of the popular reference materials in nonlinear spectroscopy, carbon disulfide (CS_2) has been the subject of numerous studies, but the reported values of n_2 taken from references over the past decades [3–19], as shown in Fig. 1, vary by over 2 orders of magnitude, depending on the experimental methods, pulse widths used, and interpretation of data. This large discrepancy arises in part from the noninstantaneous nuclear nonlinearity, present in all molecular liquids, which complicates the temporal NLO response of molecular solvents, resulting in an effective NLR coefficient, $n_{2,\mathrm{eff}}$, which depends on the pulse width [20–25].

In our study of CS_2 [20,25], we developed a methodology to fully resolve the NLO response functions using our recently developed beam-deflection (BD) technique. By investigating the polarization dependence, BD allows us to separate the bound-electronic and nuclear contributions to NLR without using very short pulses, as has been required in earlier experiments based on the optical Kerr-effect (OKE) technique, which measures the induced birefringence [22–24,26–28]. As discussed in [20,23,24], we decompose the overall response into a nearly instantaneous NLR, which originates from the bound-electronic response, and three major noninstantaneous mechanisms due to nuclear motions, namely, collision, libration, and diffusive reorientation. These mechanisms lead to a time-dependent third-order response, giving a change of refractive index that is linear in irradiance. Some selected solvents were briefly investigated in our previous work [21].

The usefulness of the response function is that it can be used to predict and interpret the outcomes of other NLO experiments over a wide range of pulse widths. For example, for CS_2, the response functions determined from our BD measurements in [20,25] have successfully predicted the pulse-width dependence of $n_{2,\mathrm{eff}}$ measured from Z-scan [20,29], as well as the results from

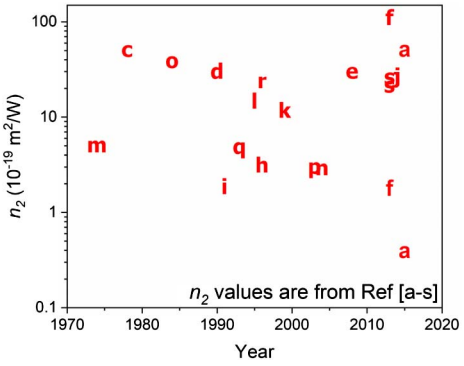

Fig. 1. Survey of literature values reported for CS_2. The letters represent references of [3–19], i.e., a: [3], c–f: [4–7], and h–s: [8–19].

other experiments, including degenerate four-wave mixing (DFWM) [20] and optical limiting [30]. In a recent study, our NLO response functions have also been used to interpret the results of mid-infrared supercontinuum generation from CS_2-core optical fibers, which helps us understand new hybrid soliton dynamics as a result of the noninstantaneous NLR of CS_2 [31,32]. Recently, seven solvents (also included in this work) were studied along with CS_2 using nonlinear ellipse rotation (NER) experiments [33,34] for a range of pulse widths, from which predictions of $n_{2,\mathrm{eff}}$ are given using an empirical model [29]. To open up more possibilities for other materials to be used in NLO applications, we follow the same BD methodology as [20,25] to perform extensive experimental characterizations on the third-order NLO response functions for 24 widely used organic solvents, as listed in Table 1. These results serve as accurate references for NLR applications using these materials and will be useful to all nonlinear optics researchers, including chemists performing studies of the NLO properties of organic dyes in solution.

In this paper, we first briefly review the physical origins of the nonlinear interactions for molecular liquids, as well as the principles of the BD technique [20,24,35]. BD measurements are performed on these 23 solvents, along with CS_2, under identical experimental conditions. By comparing the measured nonlinearities from different solvents, explanations are given from the standpoint of their molecular structures, which provide insight to help determine structure-property relations. The experimental results of the measured magnitude of the reorientational NLR are compared to the theoretical values derived from the linear polarizability tensors where the Lorentz–Lorenz local-field correction is considered. Finally, using these response functions, the pulse-width dependence of $n_{2,\mathrm{eff}}$ can be used to predict the outcomes of other experiments, such as Z-scan. Knowing the NLO response function may allow engineering of the NLR properties of solutions or suspensions, for example, mixing self-focusing and self-defocusing materials to obtain zero $n_{2,\mathrm{eff}}$ at a specific pulse width.

2. THEORY

For typical molecular liquids, the mechanisms governing the refractive index change are the combined bound-electronic and several major nuclear contributions. Light induces both linear and nonlinear polarizations in the molecules, where the second hyperpolarizability, γ, is associated with the polarization proportional to the third order of the field, as defined in [36]. For isotropic liquids, where the molecules are randomly oriented, NLR due to bound electrons can be derived from $\mathrm{Re}[\langle\gamma\rangle]$, where $\langle\cdot\rangle$ indicates orientational (angular) averaging. The bound-electronic response is fast compared to the femtosecond pulses used and can be treated as instantaneous. In lossless media, it can be described by a nonlinear refractive index [2,36,37]:

$$n_{2,el} = \frac{3}{4}\frac{N}{n_p n_e \varepsilon_0^2 c} f^{(3)} \mathrm{Re}[\langle\gamma\rangle], \tag{1}$$

where N is the number density of molecules, n_p and n_e the (real) linear refractive indices of probe and excitation in BD measurements, ε_0 is the vacuum permittivity, c is the speed of light in vacuum, and $f^{(3)} = ((n_e^2+2)/3)^2((n_p^2+2)/3)^2$ is the Lorentz–Lorenz local-field correction factor for third-order nonlinearities [1,2].

Besides the bound-electronic NLR, optically induced molecular reorientation can also give rise to a refractive index change. As the optical field polarizes the anisotropic molecule by inducing a dipole moment that may not be in the same direction as the incident field, the molecule experiences a torque to align it towards the field direction. This changes the net degree of orientation from its initial random angular distribution, resulting in a change in the refractive index due to the polarizability anisotropy of the molecules. The induced polarization can be derived from the anisotropic polarizability tensor by considering an angular probability of $\exp(-\bar{V}/k_B T)$, where $\bar{V}$ is the alignment energy from the incident field; the Boltzmann constant, k_B, and temperature, T, together account for the thermal energy that tends to return the system to a random distribution in angle. Following [1,2], the nonlinear refractive index $n_{2,d}$ due to this diffusive reorientational effect can be written as

$$n_{2,d} = \frac{N}{n_p n_e \varepsilon_0^2 c}[f_p^{(1)} f_e^{(1)}]^2 \frac{\Delta\alpha_e \Delta\alpha_p}{45 k_B T}, \tag{2}$$

where $f_p^{(1)} = (n_p^2+2)/3$ and $f_e^{(1)} = (n_e^2+2)/3$ are the first-order Lorentz–Lorenz local-field correction factors at the wavelength of probe and excitation, respectively. Here, we define $\Delta\alpha_i = \sqrt{\alpha_{\bar{x}\bar{x},i}^2 + \alpha_{\bar{y}\bar{y},i}^2 + \alpha_{\bar{z}\bar{z},i}^2 - \alpha_{\bar{x}\bar{x},i}\alpha_{\bar{z}\bar{z},i} - \alpha_{\bar{x}\bar{x},i}\alpha_{\bar{y}\bar{y},i} - \alpha_{\bar{y}\bar{y},i}\alpha_{\bar{z}\bar{z},i}}$ as the effective polarizability anisotropy, where $\alpha_{\bar{x}\bar{x}}$, $\alpha_{\bar{y}\bar{y}}$ and $\alpha_{\bar{z}\bar{z}}$ are the anisotropic polarizabilities in the molecular frame $(\bar{x},\bar{y},\bar{z})$, subscript i denotes the wavelength dependence, which reduces to $\alpha_{\bar{z}\bar{z},i} - \alpha_{\bar{x}\bar{x},i}$ for a linear molecule, where $\alpha_{\bar{y}\bar{y},i} = \alpha_{\bar{x}\bar{x},i}$. With a knowledge of the linear polarizability tensor, the theoretical $n_{2,d}$ calculated from Eq. (2) allows direct comparison to the $n_{2,d}$ measured in BD experiments. Unlike the (nearly) instantaneous bound-electronic response, reorientation is a dynamic effect and alters the refractive index in a noninstantaneous (slow) manner that depends on the parameters related to nuclear motion, such as the momenta of inertia and viscosity.

As thoroughly discussed in [20,23,24], the major optically induced nuclear mechanisms, other than diffusive reorientation that may change the refractive index of solvents are molecular libration, collision, and vibration. Following [20,25], their noninstantaneous responses are modeled using a nonlinear refractive

Table 1. Fit Parameters of Nonlinear Response Function of Solvents[a]

Family	Solvent	$n_{2,el}$	$n_{2,c}$	$\tau_{r,c}$ $\tau_{f,c}$	$n_{2,I}$	ω_0 σ	$\tau_{f,I}$	$n_{2,d}$	$\tau_{r,d}$ $\tau_{f,d}$
Benzene derivative	toluene	0.60	0.12	0.25 0.2	1.2	11 8	0.35	3.0	0.25(5) 2.1
	nitrobenzene	0.60	0.35	0.2 0.1	1.7	5 9	0.4	5.0	0.1 3.5
	benzene	0.60	0.25	0.25 0.2	1.2	11 8	0.25	2.3	0.1 1.5(4)
	p-xylene	0.62	0.20	0.25 0.2	1.1	11 6	0.35	3.3	0.25 2.6
	pyridine	0.60	0.05	0.25 0.1	1.5	12 8	0.35	3.1	0.25 1.8
	o-dichlorobenzene	0.60	0.30	0.20(5) 0.20(5)	1.0	3 10	0.15(5)	3.2	0.1 2.5
Haloalkane	dichloromethane	0.30	0.05	0.2 0.1	0.4	7 4	0.25	0.75	0.1 1.8
	chloroform	0.41	0.08	0.1 0.1	0.4	5 2	0.25	0.75	0.25 1.8
	CCl_4	0.48	0.20	0.1 0.15(5)	0	– –	–	0	– –
Ketone	acetone	0.40	0.05	0.1 0.15(5)	0.30	5 6	0.2	0.45	0.1 1.5
Nitrile	acetonitrile	0.35	0.05	0.1 0.15(5)	0.25	5 6	0.2	0.40	0.1 1.8
Formamide	DMF	0.40	0.15	0.1 0.15(10)	0.40	8 6	0.35	1.1	0.1 2.0
Ester	butyl salicylate	0.38	0.25	0.2 0.1	0.70	5 9	0.45	1.3	0.1 2.5
Ether	tetrahydrofuran	0.32	0.10	0.2 0.15(5)	0.12	4 8	0.35	0.08	0.1 2.0
Alkane	hexane	0.32	0.10	0.2 0.1	0.08	3 5	0.15(5)	0.20	0.20(5) 2.0
	cyclohexane	0.35	0.10	0.2 0.1	0.07	5 4	0.35	0.07	0.2(1) 1.5
Alcohol	methanol	0.30	0.10	0.2 0.2	0.04	8 4	0.35	<0.05	– 0.2
	1-octanol	0.40	0.06	0.2 0.1	0.03	2 2	0.15(10)	<0.06	– –
	1-butanol	0.33	0.06	0.2 0.1	0.05	3 2	0.15(10)	<0.07	– –
	ethanol	0.32	0.06	0.2 0.1	0.04	4 6	0.15(10)	<0.05	– –
Others	CS_2 [20,25]	1.50	1.0	0.15(5) 0.14(5)	7.6	8.5	0.45(10) 5	18	0.15(5) 1.61(5)
	dimethyl sulfoxide	0.45	0.13	0.4 0.15(5)	0.14	4 6	0.25	0.1	0.1 2.5
	D_2O	0.28	0.05	0.2 0.15(10)	0.04	2 2	0.1	<0.03	– –
	H_2O	0.25	0.03	0.2 0.15(10)	0.04	2 2	0.1(1)	<0.05	– –

[a] $n_{2,m}$ are given in the units of 10^{-19} m^2/W with ~20% estimated errors from uncertainty in irradiance; $\tau_{r,m}$ and $\tau_{f,m}$ are given in units of ps, errors in $\tau_{f,d}$ are ±500 fs, and those in all others are either ±50% or 100 fs (whichever is less) unless stated; ω_0 and σ are given in units of ps^{-1}, errors of ±50% or 2 ps^{-1} (whichever is less) unless stated.

index $n_{2,m}$ and a normalized response function $r_m(t)$, with $\int_{-\infty}^{\infty} r_m(t)\mathrm{d}t = 1$, where the subscript m indicates the mechanism. $r_d(t)$, for diffusive reorientation, takes the form of an exponential rise and fall, with time constants $\tau_{r,d}$ and $\tau_{f,d}$, respectively. Initiated by a torque applied by the external field, libration is an oscillatory rocking motion due to interactions with neighboring molecules. The librational response is modeled using a quantum harmonic oscillator with an antisymmetrized Gaussian distribution function with the center frequency ω_0 and bandwidth σ [22,38]. Libration arises from the same source as the diffusive reorientation and has the same symmetry. Additionally, the field-induced dipole will reradiate an electric field, which will affect its neighboring molecules by distorting their polarizabilities, thus giving a refractive index change. This is referred to as collision-induced NLR, which is modeled using an exponential rise and fall for its response function [23]. Vibrational motion can

be excited by a broadband femtosecond pulse through the stimulated Raman effect, provided the corresponding vibrational mode is Raman-active and the excitation pulse is comparable to the vibrational period. The response function of NLR from nuclear vibration takes the form of a damped oscillation at frequency ω_v, with a decay constant $\tau_{f,v}$.

Following the methodology in [20,23,39,40], these nuclear contributions are treated as linearly independent, giving the combined response function $R(t) = \sum_m n_{2,m} r_m(t)$. Together with the bound-electronic NLR, this leads to an irradiance- and time-dependent third-order response, yielding a change of refractive index linear in the excitation irradiance $I(t)$ as

$$\Delta n(t) = 2n_{2,el} I_e(t) + \sum_m \left(n_{2,m} \int_{-\infty}^{\infty} r_m(t - t') I_e(t') \mathrm{d}t' \right). \quad (3)$$

3. POLARIZATION-RESOLVED BD

The BD technique [35] used to determine the NLO response functions of solvents is a highly sensitive excite-probe technique, simultaneously measuring the absolute magnitude, sign, and temporal dynamics of both NLR and absorption. It has been shown that BD is capable of measuring a nonlinear phase change as small as 0.3 mrad (optical path length change of $\lambda/20{,}000$). Previously, BD had been extensively used to investigate ultrafast nonlinearities in various material systems: the NLR in fused silica [35], NLO response function in CS_2 [41], nondegenerate NLR in semiconductors [42], NLR transients in molecular gases [41], and possible magneto-electric nonlinearities in solvents [43]. The principle of BD has been explicitly described elsewhere [20,35]. Described briefly, optical pulses are used as excitation to create an index gradient via ultrafast NLR, deflecting the temporally delayed probe pulse with a small angle. This principle has been employed in an earlier experiment where the BD was induced by a temporal prism formed by a triangular area-modulated excitation beam [44]. In our experiment, the index gradient follows the spatial irradiance distribution of the excitation beam, i.e., Gaussian, and the deflection of the probe is measured by using a segmented detector by taking the difference of the energy, ΔE, falling on the left and right halves, as illustrated in Fig. 2. The normalized BD signal, $\Delta E/E$, where E is the total transmitted probe-pulse energy, is directly proportional to the Δn temporally averaged over the probe pulse and tells the sign of NLR from the deflection direction without the implementation of optical heterodyne detection, as is needed in OKE and DFWM experiments.

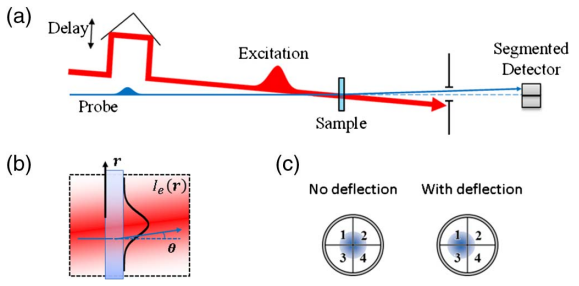

Fig. 2. (a) Schematics of BD setup; (b) spatial irradiance distribution of the excitation beam (red) and overlapping geometry with the probe beam (blue) at the sample plane; (c) positions of probe beam on segmented quad-cell detector without and with deflection.

By varying the angle θ between the polarizations of excitation and probe, BD measures the tensor symmetries of third-order nonlinearities. This allows separation of bound-electronic response from some of the nuclear contributions, as they follow different polarization dependences [35,41,42]. Within the Kleinman (low-frequency) limit [1,2], bound-electronic, collisional, and vibrational responses follow isotropic symmetry, giving $n_{2,\parallel}^{\mathrm{iso}}/n_{2,\perp}^{\mathrm{iso}} = 3$ for parallel $\parallel$ and perpendicular $\perp$ polarizations; librational and diffusive reorientational effects arise from the same field-induced torque and follow the reorientational symmetry, giving $n_{2,\parallel}^{\mathrm{re}}/n_{2,\perp}^{\mathrm{re}} = -2$. At the magic angle, $\theta = 54.7°$, the librational and diffusive reorientational contributions vanish, making possible the determination of $n_{2,el}$ as well as $\mathrm{Re}[\langle\gamma\rangle]$, along with a relatively small and delayed collisional response. Unlike other techniques such as OKE, where short femtosecond pulses, e.g., ~50 fs, are needed to separate different contributions based on temporal responses [22–24,26,27], the polarization-resolved BD allows us to unambiguously determine bound-electronic NLR, even with pulse widths longer than the rise time of nuclear responses.

BD measurements are performed using 21 μJ, 150 fs (FWHM) excitation pulses at a wavelength of 800 nm directly from a Ti:sapphire amplified system with a repetition rate of 1 kHz. A portion of the excitation is used to generate a white-light continuum by focusing into a 1 cm quartz cuvette filled with water, which is then spectrally filtered by a narrow bandpass interference filter ($\Delta\lambda \sim 10$ nm) at 700 nm to use as the probe. The excitation and probe are focused to 290 μm and 40 μm ($\mathrm{HW}1/e^2M$), respectively, at the sample. Deflection of the probe is detected by a quad-segmented Si photodiode (OSI QD50-0-SD) placed 25 cm behind the sample. The 24 solvents are all measured in 1 mm path length fused silica cuvettes under identical experimental conditions, and the contribution from the cuvette is measured separately and subtracted from the signal for each polarization.

Note that the wavelengths of the excitation and probe are chosen to be slightly nondegenerate to avoid coherent artifacts common in degenerate experiments [45]. Although the wavelengths are close enough to keep the reduction of temporal resolution caused by group velocity mismatch (GVM) to a minimum, we use the methodology developed in [41,46] to take into account any GVM in our analysis to obtain precise fits of the data.

4. RESULTS AND DISCUSSION

As an example of how to extract the parameters of the NLO response functions from the polarization-resolved BD measurements, the measured signal, $\Delta E/E$, of benzene is shown in Fig. 3(a) as a function of delay with parallel, perpendicular, and magic-angle polarization combinations. Benzene is an aromatic molecule, with a planar structure such that the polarizabilities parallel to the ring plane are much larger than in the perpendicular direction [47]. The linear polarizabilities of benzene can be found in Table 2. Since benzene has a relatively large anisotropy, much like CS_2 [35,41], the libration and diffusive reorientation contribute considerably to the NLR.

In the parallel polarized case, the instantaneous bound-electronic response is followed by a quickly damped librational response and then a slow exponential decaying component from molecular reorientation that dominates at long delays. The

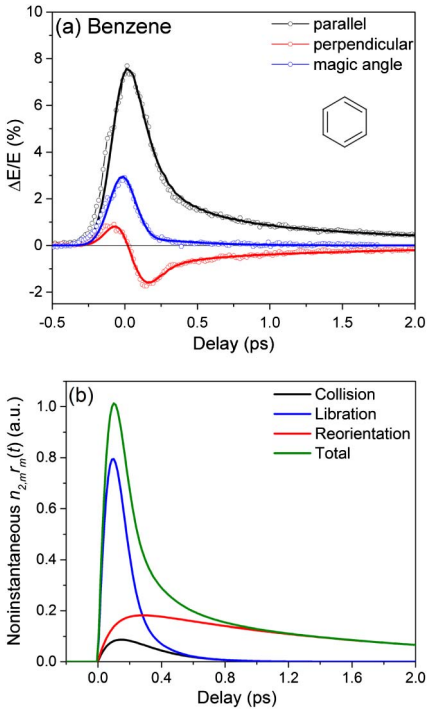

Fig. 3. (a) Data (circles) and fit (curves) of BD measurement of benzene for parallel (black), perpendicular (red), and magic-angle (blue) polarizations; (b) response function for each nuclear mechanism using the fit parameters of benzene in Table 1.

perpendicular polarization data are positive around zero delay, mainly due to the bound-electronic response and then rapidly become negative due to the tensor symmetry of librational and reorientational NLR, which decays at longer delays. At the magic angle, neither the librational nor the reorientational responses affect the probe, so $\Delta E/E$ nearly follows the cross-correlation of the excitation and probe pulses, with an additional small noninstantaneous component due to the collision-induced mechanism [51–53].

The parameters of NLO response function can thus be extracted from the fit of the data. First, bound-electronic and collisional responses are determined by fitting the slightly asymmetric signal from the magic-angle polarization. We compare the measured $n_{2,el}$ of benzene to the reported values in the literature using third-harmonic generation [54] and field-induced second-harmonic generation [55] techniques and found agreement within the experimental errors. Then, the librational and reorientational responses are be found by simultaneously fitting the parallel and perpendicular polarization data. The minor discrepancy between data and fits may come from noise sources such as laser fluctuations, as well as the subtraction of cuvette contributions. We do not observe a vibrational component in benzene, since the bandwidth of the excitation pulse does not overlap with the first vibrational transition. Figure 3(b) plots the normalized response functions for all the noninstantaneous components using the fit parameters given in Table 1, which consist of a fast-rising and rapidly damped librational component, a relatively small response due to the collisional-induced mechanism, and a slow decaying (>1 ps) response due to diffusive reorientation. Summing up, the three responses result in a maximum ~110 fs after zero delay. Together with the bound-electronics response, we construct the total NLO response function of benzene.

We have also performed BD measurements for six benzene derivatives, of which the results for toluene, *p*-xylene, pyridine, nitrobenzene, *o*-dichlorobenzene, and butyl salicylate are shown in Fig. 4. In general, the benzene moiety plays a significant role in the overall nonlinearity of the molecule, but effects from certain substitutions are also considerable. The effects from methyl-group substitutions are relatively small in molecules such as toluene and *p*-xylene, for which we obtain similar values of $n_{2,el}$ as benzene, which suggests a negligible effect from methyl substitutions. However, we observe that $n_{2,d}$ becomes slightly larger with increasing numbers of methyl groups, i.e., $n_{2,d}$ (*p*-xylene) $>n_{2,d}$(toluene) $>n_{2,d}$(benzene), which is probably attributed to the increase of effective polarizability anisotropy [47]. Similar effects are observed for pyridine, which is structurally and electronically similar to benzene by the exchange of one of the carbon-ring atoms with a nitrogen. However, for more heavily substituted benzene derivatives, we observe the reorientation-related NLR responses to be significantly altered. For example, in *o*-dichlorobenzene, a significant difference appears in the changes of the resonance frequency and bandwidth of the librational motion. For nitrobenzene, we measured a $n_{2,d}$ ~2.2 × larger than that of benzene, along with a longer diffusive reorientational lifetime

Table 2. Reorientational $n_{2,d}$ Comparison between Theoretical and Experimental Values[a]

Solvent	$\alpha_{\bar{x}\bar{x}}$	$\alpha_{\bar{y}\bar{y}}$	$\alpha_{\bar{z}\bar{z}}$	$[f_p^{(1)}f_e^{(1)}]^2$	Theory $n_{2,d}$	Theory $n_{2,d}/[f_p^{(1)}f_e^{(1)}]^2$	Exp. $n_{2,d}$
CS_2[b]	6.2	6.2	16.8	5.3	54.3	10.2	18.0 [20]
Benzene[b]	7.3	13.1	13.1	3.8	8.9	2.3	2.3
p-Xylene[c]	9.8	17.3	20.2	4.0	16.9	4.3	3.3
o-dichlorobenzene[c]	10.0	16.6	20.7	4.6	20.4	4.4	3.2
Pyridine[c]	6.4	12.0	13.2	4.1	12.2	3.0	3.1
Toluene[c]	8.2	15.1	17.2	4.0	15.5	3.8	3.0
Nitrobenzene[c]	8.6	14.7	19.8	4.5	23.7	5.2	5.0
Dichloromethane[d]	5.6	6.7	9.3	3.3	3.7	1.1	0.75
Chloroform[d]	7.5	10.5	10.5	3.4	2.5	0.73	0.75
Acetone[d]	5.4	7.9	7.9	2.7	1.6	0.6	0.45
Acetonitrile[d]	4.3	4.3	6.4	2.6	1.7	0.65	0.4
Ethanol[d]	4.9	5.4	6.3	2.8	0.5	0.18	<0.05
Methanol[d]	2.9	3.6	4.5	2.5	0.9	0.37	<0.05

[a]Theoretical $n_{2,d}$ is calculated from Eq. (2), and the experimental $n_{2,d}$ is from Table 1, with the units of 10^{-19} m^2/W.
[b]$\alpha_{\bar{x}\bar{x}}$, $\alpha_{\bar{y}\bar{y}}$ and $\alpha_{\bar{z}\bar{z}}$ are experimental values from [49] and are given in the units of 10^{-40} Fm^2.
[c]$\alpha_{\bar{x}\bar{x}}$, $\alpha_{\bar{y}\bar{y}}$ and $\alpha_{\bar{z}\bar{z}}$ are experimental values from [50] and are given in the units of 10^{-40} Fm^2.
[d]$\alpha_{\bar{x}\bar{x}}$, $\alpha_{\bar{y}\bar{y}}$ and $\alpha_{\bar{z}\bar{z}}$ are experimental values from [48] and are given in the units of 10^{-40} Fm^2.

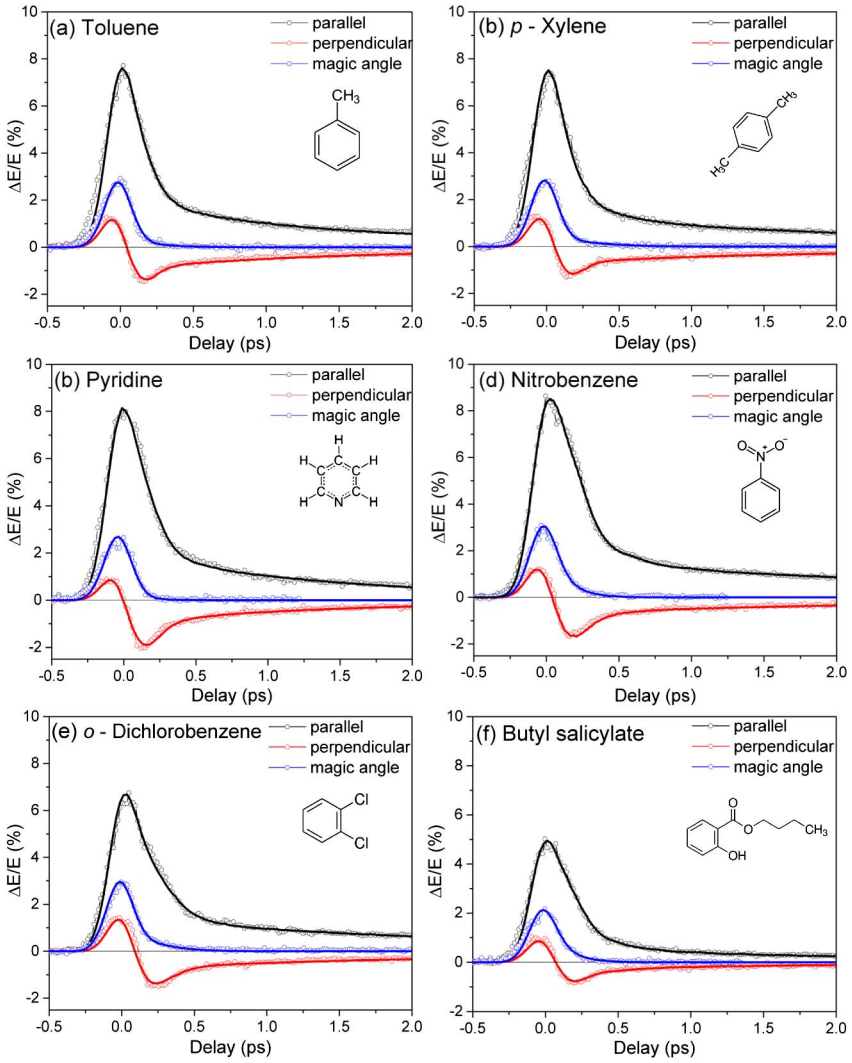

Fig. 4. BD measurements (circles) with fits (lines) of benzene derivatives including (a) toluene, (b) *p*-xylene, (c) pyridine, (d) nitrobenzene, (e) *o*-dichlorobenzene and (f) butyl salicylate for parallel (black), perpendicular (red), and magic-angle (blue) polarizations.

$\tau_{f,d}$. Despite the large changes in librational and reorientational responses, their $n_{2,el}$ values measured from the magic-angle polarization data are measured to be the same as that of benzene within measurement error, indicating that the electronic interactions introduced from these substitutions are small. However, a smaller $n_{2,el}$ is measured when benzene includes an ester group substitution, i.e., butyl salicylate. To fully understand the effects of benzene substitutions on the bound-electronic NLR, rigorous analysis of the electronic structure and calculations of the second hyperpolarizabilities would be needed [56–58].

BD measurements of dichloromethane, chloroform, and carbon tetrachloride (CCl_4) are shown in Fig. 5. These three molecules all have similar tetrahedral geometries, but with different numbers of *H* (or Cl) atoms, which affect both electronic and nuclear NLR. As shown in Figs. 5(a) and 5(b), dichloromethane and chloroform show similar noninstantaneous responses that decay within the first several picoseconds. We attribute this to their asymmetrical structures, as shown in the insets, which lead to the anisotropic polarizabilities listed in Table 2 [47]. The reorientation-related responses vanish in CCl_4, shown in Fig. 5(c), which is a highly symmetric molecule with zero polarizability anisotropy, i.e., $\alpha_{\overline{xx}} = \alpha_{\overline{yy}} = \alpha_{\overline{zz}}$, resulting in $n_{2,d} = 0$, based on Eq. (2). Therefore, the fits only consider a bound-electronic and a relatively small collision-induced mechanism. Using a shorter excitation pulse width of 50 fs leads to the excitation of the Raman-active vibrational mode at the frequency of 218 cm^{-1} [59], corresponding to the "scissor" vibrational motion. Figure 5(d) shows the BD measurement with a 115 fs probe polarized parallel to the excitation of the combination of CCl_4 and cuvette. The oscillatory signal is fit with a single frequency $\omega_v =$ 40.8 rad/s (218 cm^{-1}) with a decay constant $\tau_{f,v} = 1.2$ ps and an NLR coefficient of $n_{2,v} = -0.05 \times 10^{-19}$ m^2/W, where the subscript *v* denotes the vibrational mechanism. Note the NLR due to molecular vibration is relatively small compared to other nuclear mechanisms in CCl_4. Comparing the bound-electronic NLR, $n_{2,el}$ increases with the number of C–Cl bonds, i.e., $n_{2,el}(CCl_4) > n_{2,el}(CHCl_3) > n_{2,el}(CH_2Cl_2)$. This is consistent with a higher second hyperpolarizability for the C–Cl bond than for the C–H bond [60].

Molecules with asymmetric structures do not necessarily show large librational and reorientational NLR. The magnitudes of these responses are closely related to the value of polarizability

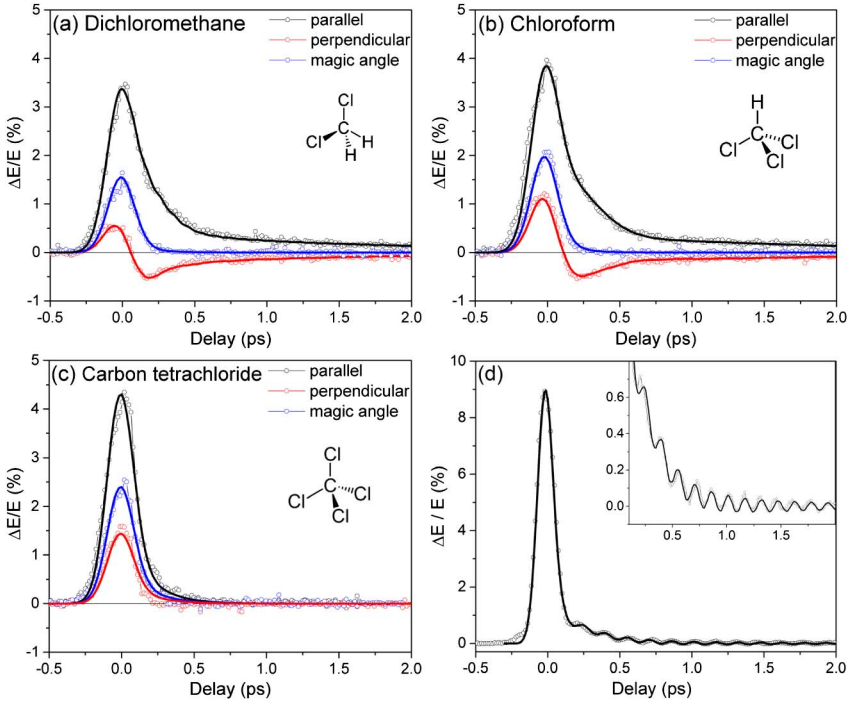

Fig. 5. BD measurements (circles) with fits (lines). (a) Dichloromethane, (b) chloroform, and (c) CCl_4 for parallel (black), perpendicular (red), and magic-angle (blue) polarizations; (d) measured CCl_4 response excited with shorter pulse width with parallel polarization (circles), with a fit including the vibrational response (inset shows the vibrational component enlarged).

anisotropy. For example, like benzene, cyclohexane is a cyclic molecule with six carbon atoms, but they are combined with single bonds without π electrons, which leads to a small anisotropy in its polarizability [47].

Also, cyclohexane has a twisted structure, i.e., chair or boat conformations, which may also result in a smaller anisotropy. As shown in Fig. 6(a), $n_{2,l}$ and $n_{2,d}$ for cyclohexane are much smaller than those of benzene [compare with Fig. 3(a)]. Alcohols are all asymmetric molecules, but their responses are dominated by bound-electronic NLR with some small noninstantaneous components that decay in several hundred femtoseconds. As an example, the results for 1-octanol are shown in Fig. 6(b). The noninstantaneous responses include collisional NLR as well as a very small reorientation-related response observed from the difference between parallel and perpendicular polarizations. Similar signals are also observed for methanol, ethanol, and 1-butanol, as shown in Figs. S1(a)–S1(c). We attribute it to librational NLR, as the ~150 fs decay time is too fast for typical diffusive reorientational responses. Along with the fit parameters in Table 1, an upper limit of $n_{2,d}$ is estimated, based on experimental noise at longer delay. Similar to cyclohexane, this small reorientational NLR can be attributed to the fact that alcohols are single-bonded molecules without conjugation, so the polarizability along the molecular axis is not significantly larger than in other directions [47], yielding a small anisotropy. As shown in Table 2, the theoretically predicted $n_{2,d}$ of ethanol, calculated from the polarizability tensor using Eq. (2), is ~8 × smaller than that of dichloromethane and ~24 × smaller than that of benzene.

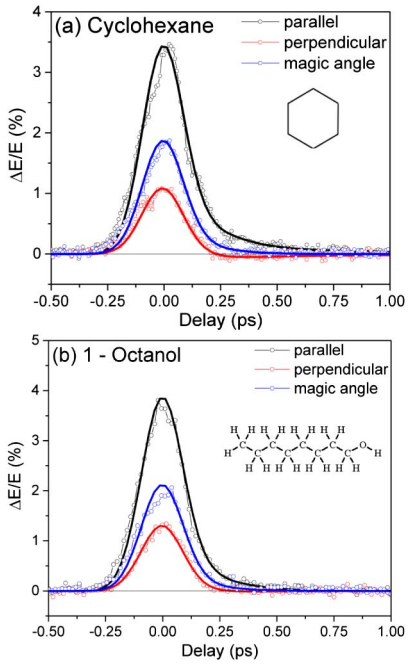

Fig. 6. BD measurements (circles) with fits (lines). (a) Cyclohexane and (b) 1-octanol for parallel (black), perpendicular (red), and magic-angle (blue) polarizations.

Similar responses are measured in other solvents, including dimethyl sulfoxide, hexane, tetrahydrofuran, water, and heavy water, as shown in Figs. S1(d)–S1(h), which all have an asymmetric structure but with the bound-electronic response dominating their NLR. The other solvents included in this study are acetone, acetonitrile, and dimethylformamide (DMF). The BD results (see Figs. S1(i)–S1(k) and Table 1) show their NLO response functions have contributions from all three major nuclear mechanisms.

The NLO response function of solvents measured from BD experiments is useful to compare to the values predicted

by theoretical models. From the measured $n_{2,el}$, the electronic second hyperpolarizability Re[$\langle\gamma\rangle$] may be derived from Eq. (1), which includes the third-order Lorentz–Lorenz local-field correction factor $f^{(3)}$, which serves as a comparison of Re[$\langle\gamma\rangle$] measured in the gas phase, where $f^{(3)} \sim 1$. In our previous studies [20,25,36,41], we measured Re[$\langle\gamma\rangle$] of CS_2 molecules in both gas and liquid phase, which showed agreement with a local-field factor of $f^{(3)} = 5.35$ in the liquid phase. Therefore, assuming local-field theory is correct, gas and liquid phase CS_2 has the same value of second hyperpolarizability. Gas-phase measurements on the other solvents will provide more comparisons of Re[$\langle\gamma\rangle$] to their liquid phase counterparts as derived from $n_{2,el}$ in Table 1, which should indicate how third-order local-field theory works for other molecules, including polar molecules.

We may compare measurements of $n_{2,d}$ to theoretical values calculated via Eq. (2) in Table 2 using polarizability tensor elements $\alpha_{\overline{xx}}$, $\alpha_{\overline{yy}}$, and $\alpha_{\overline{zz}}$ from experimentally measured values in [48–50]. Here we take $\Delta\alpha_e = \Delta\alpha_p$, as the wavelengths used for excitation and probe are nearly degenerate in this experiment, and their dispersion is nearly flat. Note that the theoretical prediction of linear refractive index using these tensor elements has shown good agreement with experimental results when the Lorentz–Lorenz local-field correction factor is considered. However, Eq. (2) itself tends to significantly overestimate $n_{2,d}$ by a factor of 3–6, depending on the solvent. Surprisingly, neglecting the Lorentz–Lorenz local-field correction factor, i.e., $n_{2,d}/[f_p^{(1)} f_e^{(1)}]^2$, results in better agreement with our experimental measurements. This disagreement is likely due to the simplified theory [1,2] not taking into account the full molecular dynamics and the impact of liquids correlation on the internal field. It has been suggested that the simple Lorentz internal field assumed in the theory is inadequate, and an accurate picture requires additional terms in Eq. (2) to take into account the effect from correlated distribution of molecules [61]. With the current theory, the field-induced torque and thermal relaxation experienced by the molecule results only in diffusive reorientation and does not include many-body effects, which give rise to librational and collisional effects. Full molecular dynamics simulations [62] may be necessary to capture the intermolecular behavior and correctly predict the NLO response function.

5. DETERMINATION OF EFFECTIVE n_2 VERSUS PULSE WIDTH

With knowledge of the NLO response function, we are able to predict the effective NLR coefficient, $n_{2,\text{eff}}$, for single-beam experiments such as Z-scan, where the index change is averaged temporally over the pulse irradiance. In [20], $n_{2,\text{eff}}$ is derived by taking into account both bound-electronic NLR and the overall response functions of the nuclear mechanisms, which yields

$$n_{2,\text{eff}} = n_{2,el} + \frac{\int_{-\infty}^{\infty} I(t) \int_{-\infty}^{\infty} R(t-t')I(t')\mathrm{d}t'\mathrm{d}t}{\int_{-\infty}^{\infty} I^2(t)\mathrm{d}t}. \quad (4)$$

This results in a pulse-width dependence of the effective NLR of the material. For very short pulses, i.e., <50 fs, only the bound-electronic nonlinearity contributes significantly ($n_{2,\text{eff}} \cong n_{2,el}$) due to its nearly instantaneous nature. For longer pulse widths, the noninstantaneous nuclear nonlinearities, particularly librational and reorientational responses, start to contribute and may even become dominant for very long pulses, which increases $n_{2,\text{eff}}$. The effect has been previously investigated for CS_2 using Z-scan with the pulse width varied over 3 orders of magnitude [20], where the pulse-width dependence of $n_{2,\text{eff}}$ was well predicted from Eq. (4) using the NLO response functions determined from BD measurements. The pulse-width dependence of $n_{2,\text{eff}}$ also helps us to understand the large discrepancies in Fig. 1 for measurements of n_2 of CS_2. If we plot these values according to the pulse width used in each of these references, the overall discrepancy between theory and experiment is greatly reduced, as seen in Fig. 7(a).

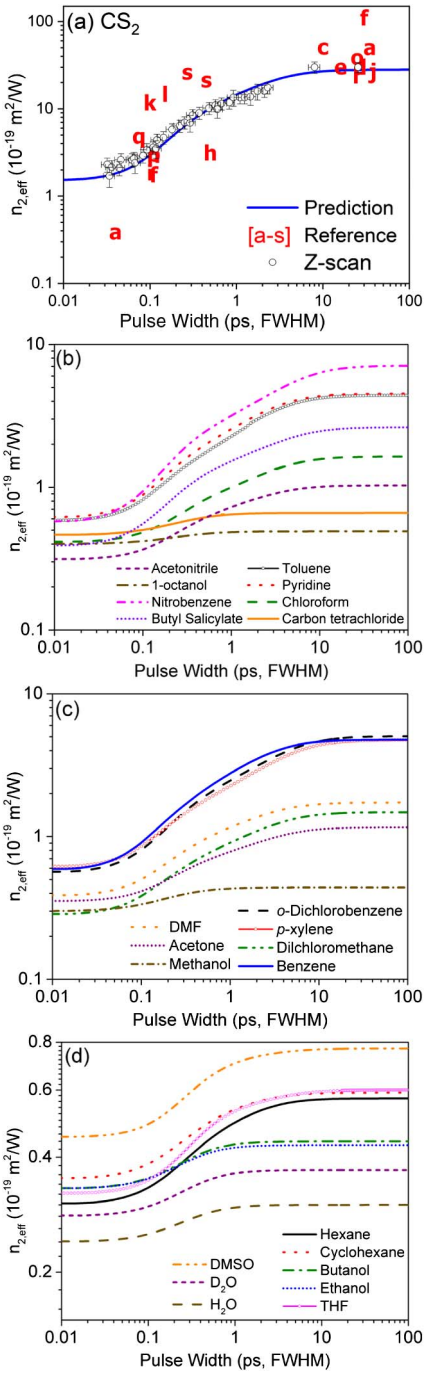

Fig. 7. Predictions of pulse-width dependent $n_{2,\text{eff}}$ of (a) CS_2 using parameters in Table 1, which is compared to Z-scan measurements in [20,25], as well as literature values a–s from references specified in the caption of Fig. 1; (b),(c) predictions of the other 23 solvent molecules using parameters in Table 1.

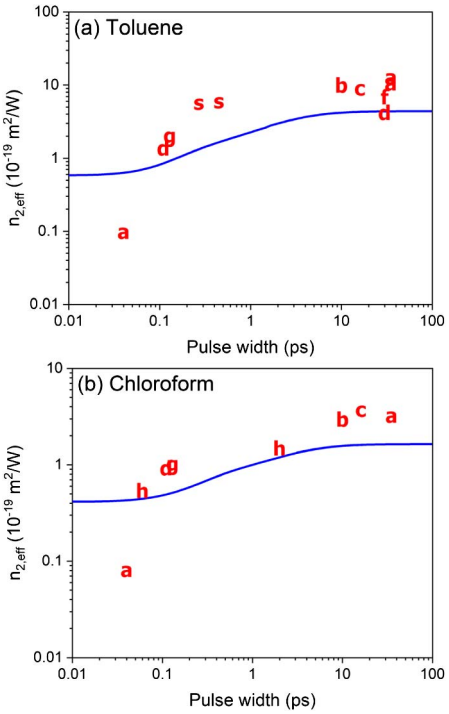

Fig. 8. Predictions (blue) of pulse-width dependent $n_{2,\mathrm{eff}}$ of (a) toluene and (b) chloroform using parameters in Table 1, which are compared to literature values a–s from references specified in the caption of Fig. 1.

Based on the same methodology, we calculate the pulse-width dependence of $n_{2,\mathrm{eff}}$ for the other 23 solvent molecules using the NLO response functions with parameters given in Table 1, as shown in Figs. 7(b)–7(d). These results represent the predictions of the outcomes of Z-scan measurements using various pulse widths. The $n_{2,\mathrm{eff}}$ of the benzene derivatives at longer pulse widths (>10 ps) increases ∼8 × over the short pulse limit, primarily owing to their large $n_{2,I}$ and $n_{2,r}$, while ∼4 × increase of $n_{2,\mathrm{eff}}$ is seen for chloroform for the same reasons. CCl_4 and alcohols with zero or negligible reorientational nonlinearities do not show a considerable increase of $n_{2,\mathrm{eff}}$ for longer pulse widths as expected from their response functions, e.g., $n_{2,\mathrm{eff}}$ of ethanol shows an increases of only ∼1.3 × for long pulse widths, which is consistent with the observation in [29]. Other NLO experiments such as Z-scan can be used to verify such predictions from BD measurements, as is shown for CS_2 [20,25].

While the literature on these solvents is less extensive than for CS_2, the same corrections can be made for literature-reported values of n_2 for these molecules. As shown in Fig. 8 for toluene and chloroform, the predictions of the pulse-width dependent $n_{2,\mathrm{eff}}$ account for the nuclear contributions using the response functions in Table 1. The comparisons of the predictions to literature values for some other solvents are shown in Fig. S2.

6. ENGINEERING THE EFFECTIVE n_2 IN SOLUTIONS

The NLO response function of solvents also helps interpret experimental results from measurements performed on solutions of organic dyes. By separating the contributions from solvent and solute, the origins of the nonlinearity for the organic molecule itself (solute) can be revealed. For example, two cyanine-like dyes,

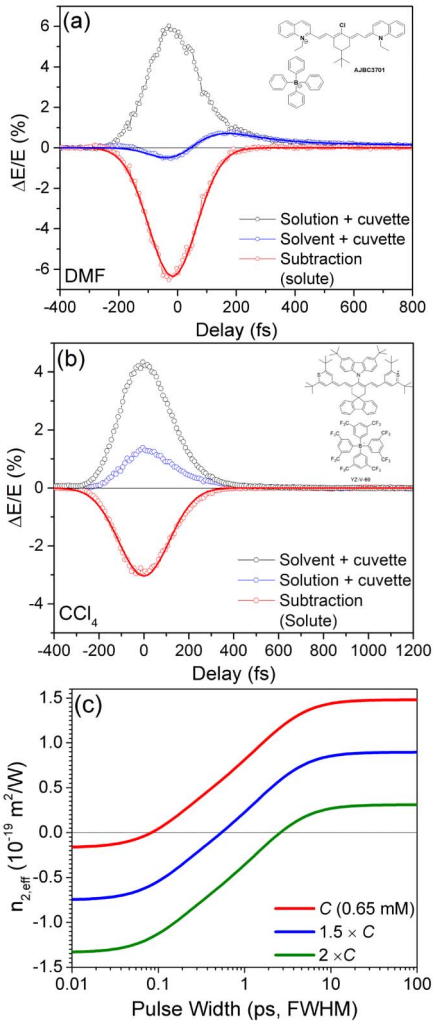

Fig. 9. BD measurements of (a) AJBC3701 in DMF solution with a fit, and (b) YZ-V-69 in CCl_4 solution (blue). The responses from the solvents with cuvette (black) are measured under identical experimental conditions. The solute signal (red circles) is from subtraction of solvent background from solution response, with a fit (red lines) considering only bound-electronic NLR. Inset shows molecular structures. (c) Predictions of pulse-width dependent $n_{2,\mathrm{eff}}$ of AJBC3701 solutions with different concentrations.

denoted as AJBC3701 and YZ-V-69, with their molecular structures shown in the inset of Figs. 9(a) and 9(b), respectively, have been extensively studied in our previous work using the dual-arm Z-scan technique [63,64]. A large and negative NLR along with a relatively small two-photon absorption is measured at wavelengths approaching their linear absorption edge, making them possible candidate materials for organic all-optical switching application [63,65–67]. To explore the physical origins of this large and negative NLR, we make two solution samples by dissolving AJBC3701 and YZ-V-69 into DMF and CCl_4, respectively, and perform BD measurements on them to resolve the temporal dynamics of the NLR. As shown in Fig. 9(a), a 0.65 mM AJBC3701 solution and a pure DMF solvent are measured under identical experimental conditions, with 4 μJ excitation pulses at the wavelength of 1250 nm at a 1 kHz repetition rate with probe pulses at 950 nm. The beam radii ($HW1/e^2M$) of excitation and probe are 470 μm

and 90 μm; pulse widths are 110 fs and 160 fs, determined from auto- and cross-correlation measurements.

The solution shows a negative signal near zero delay and switches sign to positive to reach a maximum at ~200 fs, which then decays slowly in the next several picoseconds. This signal can be understood by comparing it to the transient NLR of the pure solvent (here DMF). The initial negative signal is attributed to the combined bound-electronic NLR of AJBC3701, DMF, and the cuvette. Then the nuclear (slower) nonlinearities of DMF, i.e., librational and diffusive reorientational NLR, start to contribute and result in the following positive NLR. The complete overlap of the decaying signals between solvent and solution measurements indicates it originates solely from the reorientational relaxation of DMF. The response of the pure solute (AJBC3701) is extracted by subtracting the solution signal from the solvent background, which is negative and follows the cross-correlation of excitation and probe pulses, indicating its origin as bound-electronic NLR. We fit it with a nondegenerate NLR cross section $\delta = -3500$ GM, which is larger than the value measured from the dual-arm Z-scan at the same wavelength of the probe [63], possibly due to the intermediate-state resonance enhancement of NLR [68]. Using the nuclear components of the response function of DMF in Table 1, we fit the BD signal from the AJBC3701 solution sample in Fig. 9(a) with a negative bound-electronic NLR, i.e., $n_{2,el} = -0.17 \times 10^{-19}\ \mathrm{m}^2/W$, at this particular concentration of AJBC3701.

Similarly, we also perform BD measurements on a 0.32 mM YZ-V-69 solution with a pure CCl_4 solvent, using nearly frequency-degenerate excitation and probe pulses around the wavelength of 1200 nm, as shown in Fig. 9(b). The bandwidth is 10 nm (FWHM) for both excitation and probe pulses; the beam radii ($HW1/e^2M$) are 470 and 120 μm, and pulse widths are 150 and 220 fs. The response function of CCl_4 is dominated by bound-electronic NLR with a small noninstantaneous contribution from the collision-induced mechanism. We confirm that the large and negative NLR of YZ-V-69 also originates from the bound-electronic nonlinearity. A fit of the solute signal gives $\delta = -2500$ GM, in agreement with previous measurements by Z-scan [63].

The transient NLR of the AJBC3701 solution results in an interesting pulse-width-dependent $n_{2,\mathrm{eff}}$, as shown in Fig. 9(c). The negative bound-electronic NLR from the solute leads to a negative $n_{2,\mathrm{eff}}$ for short pulses, but a positive $n_{2,\mathrm{eff}}$ is predicted for longer pulse widths due to the slower nuclear responses of the solvent. There is a particular pulse width, i.e., 82 fs for a concentration of 0.65 mM, at which $n_{2,\mathrm{eff}}$ becomes zero. As shown in Fig. 9(c), with knowledge of the NLO response function of the solvent, the zero-crossing pulse width of $n_{2,\mathrm{eff}}$ of a solution can be engineered by varying the concentration of the solute, e.g., 536 fs and 2.6 ps, when increasing the concentration by 1.5 × and 2 ×, respectively. Unlike solid-state materials with dopants, where the negative NLR from induced carriers is usually long-lived and accompanied by large linear loss, the solutions developed here utilize the negative bound-electronic NLR from certain solutes that is nearly instantaneous, and with no linear loss.

Note, at the pulse width where $n_{2,\mathrm{eff}} \sim 0$, the rising and falling edges of the pulse still experience negative and positive phase changes [42], but the overall phase change is temporally averaged to zero. This allows for high-energy supercontinuum generation in condensed matter, where the zero $n_{2,\mathrm{eff}}$ significantly increases the critical power threshold for catastrophic self-focusing, but the nonzero first temporal derivative of $n_{2,\mathrm{eff}}$ still leads to spectral broadening via self-phase modulation.

For applications where $n_{2,\mathrm{eff}}$ is required to be nearly zero for any pulse width used, solvents such as CCl_4 and alcohols are good candidates, as the bound-electronic NLR dominates their nonlinear response [69].

7. CONCLUSION

We have experimentally determined the third-order NLO response functions for 24 solvents using our recently developed BD technique. By investigating the temporal dynamics and polarization dependence, the bound-electronic and nuclear contributions to NLR are explicitly separated. For molecules with anisotropic polarizabilities, we observe a universal temporal response of NLR, which can be decomposed into four major mechanisms, namely, a nearly instantaneous bound-electronic NLR, a fast-rising but quickly damped response due to librational motion, a relatively small noninstantaneous collision-induced component, and an exponential decaying response from molecular reorientation that dominates on longer time scales. Note that Raman-active vibrational motion may also be excited if the pulse width is short enough, which manifests as a damped oscillatory response of NLR; however, this was not thoroughly investigated in this work. In addition, for nanosecond pulses, the effects of electrostriction can become significant, which is not included in this work. We therefore put an upper limit on the pulse width of the predictive capabilities of ~1 ns.

We found the NLO response functions are closely related to their molecular structures. Benzene derivatives exhibit large librational and diffusive reorientational responses, and the benzene moiety in general plays a significant role in the overall nonlinearity. This is in part because of its aromaticity, resulting in a planar structure with a relatively larger polarizability anisotropy. Depending on the substitution groups, the nonlinear response of benzene derivatives may be altered. The results show methyl substitutions give minor effects on both electronic and reorientational NLR. But very different reorientation-related responses are measured in nitrobenzene and *o*-dichlorobenzene, and slightly smaller electronic NLR is measured in butyl salicylate. The results also indicate the magnitude of the reorientational contribution is dependent upon the linear polarizability anisotropy of the molecule. Negligible reorientational response is observed in single-bonded molecules such as alcohols and cyclohexane.

Additionally, the reorientation NLR coefficient, $n_{2,d}$, measured from polarization-resolved BD allows direct comparison to the value derived from the linear polarizability tensors with Lorentz–Lorenz local-field corrections. The comparisons based on selected solvents from Table 2 show better agreement between experiment and theory if the Lorentz–Lorenz local-field correction factor is not included. However, the full molecular dynamics and many-body effects are not taken into account in this theory. Also, the values of bound-electronic $n_{2,el}$ of these solvents are unambiguously determined from magic-angle measurements, from which the electronic second hyperpolarizability, γ, can be derived considering a third-order (nonlinear) Lorentz–Lorenz local field. These γ values measured in liquid phase can be compared to those of the isolated molecules measured in gas phase, where the local-field effect is negligible. This has been previously investigated for CS_2 [36,41], where γ is found to be equal for liquid and gas phase

measurements. The measurements of γ for other solvents in gas phase are the subject of future work.

The effective nonlinear refractive index $n_{2,\text{eff}}$ for these solvents has been calculated over a range from 10 fs to 100 ps based on the parameters of the measured response functions, which serve as predictions for other experiments such as Z-scan with various pulse widths. Significant pulse dependence, i.e., nearly an order of magnitude increase of $n_{2,\text{eff}}$ with longer pulse width, is predicted for molecules with large polarizability anisotropy, such as benzene derivatives. $n_{2,\text{eff}}$ of nonconjugated molecules such as alcohols is almost independent of the pulse width used.

With the knowledge of the NLO response function of the solvents, we are able to interpret experimental results performed on dyes in solution. We have demonstrated this for cyanine dyes dissolved in DMF and CCl_4 and confirm the bound-electronic origins of their NLR. The NLO response functions also allow us to engineer the transient NLR properties of solutions using organic dyes with a negative NLR. For example, by choosing a proper concentration of the cyanine-like dyes, one can make a solution with nearly zero $n_{2,\text{eff}}$ for a particular pulse width of interest. It will also be of interest to investigate the spectral broadening in some solutions at a certain pulse width.

We therefore establish accurate references for 24 common nonlinear solvents by offering the response function as a complete picture of their NLO properties. These response functions provide a rich database to explore the molecular structure-property relations and serve as the fingerprints for material identification or chemical sensing. In addition, the response function allows us to predict the outcomes of other NLR-related experiments on these materials and helps in optimizing the experimental parameters, such as pulse width used in the experiments or applications. The knowledge also enables developing new nonlinear solutions by engineering the transient NLR properties.

Funding. National Science Foundation (NSF) (ECCS-1202471, ECCS-1229563); Air Force Office of Scientific Research (AFOSR) (FA9550-10-1-0558); Army Research Laboratory (ARL) (W911NF-15-2-0090); UCF Pre-eminent Postdoctoral Program.

Acknowledgment. We thank David Zelmon of Air Force Research Laboratory for measuring the dispersion of several of the solvents, and Manuel R. Ferdinandus for taking the data of CCl_4. We thank Trenton R. Ensley, William M. Shensky III, and Andrew G. Mott from ARL for helpful discussions.

See Supplement 1 for supporting content.

REFERENCES

1. R. W. Boyd, *Nonlinear Optics*, 3rd ed. (Academic, 2008).
2. G. I. Stegeman and R. A. Stegeman, *Nonlinear Optics: Phenomena, Materials and Devices* (Wiley, 2012).
3. K. Iliopoulos, D. Potamianos, E. Kakkava, P. Aloukos, I. Orfanos, and S. Couris, "Ultrafast third order nonlinearities of organic solvents," Opt. Express **23**, 24171–24176 (2015).
4. P. P. Ho and R. R. Alfano, "Optical Kerr effect in liquids," Phys. Rev. A **20**, 2170–2187 (1979).
5. M. Sheik-Bahae, A. A. Said, T. H. Wei, D. J. Hagan, and E. W. Van Stryland, "Sensitive measurement of optical nonlinearities using a single beam," IEEE J. Quantum Electron. **26**, 760–769 (1990).
6. I. Rau, F. Kajzar, J. Luc, B. Sahraoui, and G. Boudebs, "Comparison of Z-scan and THG derived nonlinear index of refraction in selected organic solvents," J. Opt. Soc. Am. B **25**, 1738–1747 (2008).
7. M. Bala Murali Krishna and D. Narayana Rao, "Influence of solvent contribution on nonlinearities of near infra-red absorbing croconate and squaraine dyes with ultrafast laser excitation," J. Appl. Phys. **114**, 133103 (2013).
8. S. Couris, E. Koudoumas, F. Dong, and S. Leach, "Sub-picosecond studies of the third-order optical nonlinearities toluene solutions," J. Phys. B **29**, 5033–5041 (1996).
9. K. Minoshima, M. Taiji, and T. Kobayashi, "Femtosecond time-resolved interferometry for the determination of complex nonlinear susceptibility," Opt. Lett. **16**, 1683–1685 (1991).
10. F. Zhao, Z. Pan, C. Wang, Y. Zhou, and M. Qin, "Third-order nonlinear optical properties of an azobenzene-containing ionic liquid crystalline polymer," Opt. Quantum Electron. **46**, 1491–1498 (2014).
11. T. Kawazoe, H. Kawaguchi, J. Inoue, O. Haba, and M. Ueda, "Measurement of nonlinear refractive index by time-resolved z-scan technique," Opt. Commun. **160**, 125–129 (1999).
12. E. T. J. Nibbering, M. A. Franco, B. S. Prade, G. Grillon, C. Le Blanc, and A. Mysyrowicz, "Measurement of the nonlinear refractive index of transparent materials by spectral analysis after nonlinear propagation," Opt. Commun. **119**, 479–484 (1995).
13. M. D. Levenson and N. Bloembergen, "Dispersion of the nonlinear optical susceptibilities of organic liquids and solutions," J. Chem. Phys. **60**, 1323–1327 (1974).
14. R. A. Ganeev, A. I. Ryasnyansky, N. Ishizawa, M. Baba, M. Suzuki, M. Turu, S. Sakakibara, and H. Kuroda, "Two- and three-photon absorption in CS_2," Opt. Commun. **231**, 431–436 (2004).
15. N. Phu Xuan, J.-L. Ferrier, J. Gazengel, and G. Rivoire, "Picosecond measurements of the third order susceptibility tensor in liquids," Opt. Commun. **51**, 433–437 (1984).
16. S. Couris, M. Renard, O. Faucher, B. Lavorel, R. Chaux, E. Koudoumas, and X. Michaut, "An experimental investigation of the nonlinear refractive index (n_2) of carbon disulfide and toluene by spectral shearing interferometry and z-scan techniques," Chem. Phys. Lett. **369**, 318–324 (2003).
17. H.-S. Albrecht, P. Heist, J. Kleinschmidt, and D. V. Lap, "Ultrafast beam-deflection method and its application for measuring the transient refractive index of materials," Appl. Phys. B **57**, 193–197 (1993).
18. G. Boudebs, M. Chis, and J. P. Bourdin, "Third-order susceptibility measurements by nonlinear image processing," J. Opt. Soc. Am. B **13**, 1450–1456 (1996).
19. S. Kedenburg, A. Steinmann, R. Hegenbarth, T. Steinle, and H. Giessen, "Nonlinear refractive indices of nonlinear liquids: wavelength dependence and influence of retarded response," Appl. Phys. B **117**, 803–816 (2014).
20. M. Reichert, H. Hu, M. R. Ferdinandus, M. Seidel, P. Zhao, T. R. Ensley, D. Peceli, J. M. Reed, D. A. Fishman, S. Webster, D. J. Hagan, and E. W. Van Stryland, "Temporal, spectral, and polarization dependence of the nonlinear optical response of carbon disulfide," Optica **1**, 436–445 (2014).
21. P. Zhao, M. Reichert, T. R. Ensley, W. M. Shensky, A. G. Mott, D. J. Hagan, and E. W. Van Stryland, "Nonlinear refraction dynamics of solvents and gases," Proc. SPIE **9731**, 97310F (2016).
22. C. Kalpouzos, D. McMorrow, W. T. Lotshaw, and G. A. Kenney-Wallace, "Femtosecond laser-induced optical Kerr dynamics in CS_2/alkane binary solutions," Chem. Phys. Lett. **150**, 138–146 (1988).
23. D. McMorrow, W. T. Lotshaw, and G. A. Kenney-Wallace, "Femtosecond optical Kerr studies on the origin of the nonlinear responses in simple liquids," IEEE J. Quantum Electron. **24**, 443–454 (1988).
24. D. McMorrow, N. Thantu, V. Kleiman, J. S. Melinger, and W. T. Lotshaw, "Analysis of intermolecular coordinate contributions to third-order ultrafast spectroscopy of liquids in the harmonic oscillator limit," J. Phys. Chem. A **105**, 7960–7972 (2001).
25. M. Reichert, H. Hu, M. R. Ferdinandus, M. Seidel, P. Zhao, T. R. Ensley, D. Peceli, J. M. Reed, D. A. Fishman, S. Webster, D. J. Hagan, and E. W. Van Stryland, "Temporal, spectral, and polarization dependence of the nonlinear optical response of carbon disulfide: erratum," Optica **3**, 657–658 (2016).
26. S. Kakinuma and H. Shirota, "Dynamic Kerr effect study on six-membered-ring molecular liquids: benzene, 1,3-cyclohexadiene, 1,4-cyclohexadiene, cyclohexene, and cyclohexane," J. Phys. Chem. B **119**, 4713–4724 (2015).

27. N. Thantu and R. S. Schley, "Ultrafast third-order nonlinear optical spectroscopy of chlorinated hydrocarbons," Vib. Spectrosc. **32**, 215–223 (2003).
28. Q.-h. Gong, J.-l. Li, T.-q. Zhang, and H. Yang, "Ultrafast third-order optical nonlinearity of organic solvents investigated by subpicosecond transient optical Kerr effect," Chin. Phys. Lett. **15**, 30–31 (1998).
29. M. L. Miguez, T. G. B. De Souza, E. C. Barbano, S. C. Zilio, and L. Misoguti, "Measurement of third-order nonlinearities in selected solvents as a function of the pulse width," Opt. Express **25**, 3553–3565 (2017).
30. L. G. Holmen and M. W. Haakestad, "Optical limiting properties and z-scan measurements of carbon disulfide at 2.05 μm wavelength," J. Opt. Soc. Am. B **33**, 1655–1660 (2016).
31. M. Chemnitz, M. Gebhardt, C. Gaida, F. Stutzki, J. Kobelke, J. Limpert, A. Tünnermann, and M. A. Schmidt, "Hybrid soliton dynamics in liquid-core fibres," Nat. Commun. **8**, 42 (2017).
32. M. Chemnitz, C. Gaida, M. Gebhardt, F. Stutzki, J. Kobelke, A. Tünnermann, J. Limpert, and M. A. Schmidt, "Carbon chloride-core fibers for soliton mediated supercontinuum generation," Opt. Express **26**, 3221–3235 (2018).
33. E. C. Barbano, T. G. Bezerra de Souza, S. C. Zilio, and L. Misoguti, "Comparative study of electronic and orientational nonlinear refractive indices with nonlinear ellipse rotation measurements," J. Opt. Soc. Am. B **33**, E40–E44 (2016).
34. M. L. Miguez, E. C. Barbano, J. A. Coura, S. C. Zílio, and L. Misoguti, "Nonlinear ellipse rotation measurements in optical thick samples," Appl. Phys. B **120**, 653–658 (2015).
35. M. R. Ferdinandus, H. Hu, M. Reichert, D. J. Hagan, and E. W. Van Stryland, "Beam deflection measurement of time and polarization resolved ultrafast nonlinear refraction," Opt. Lett. **38**, 3518–3521 (2013).
36. M. Reichert, P. Zhao, J. M. Reed, T. R. Ensley, D. J. Hagan, and E. W. Van Stryland, "Beam deflection measurement of bound-electronic and rotational nonlinear refraction in molecular gases," Opt. Express **23**, 22224–22237 (2015).
37. P. N. Butcher and D. Cotter, *The Elements of Nonlinear Optics* (Cambridge University, 1990).
38. J. S. Friedman and C. Y. She, "The effects of molecular geometry on the depolarized stimulated gain spectra of simple liquids," J. Chem. Phys. **99**, 4960–4969 (1993).
39. H. Tzer-Hsiang, H. Chia-Chen, W. Tai-Huei, S. Chang, Y. Shih-Ming, T. Chi-Pin, L. Ray-Tang, C. Kuo, X. Tong, T. Wan-Sun, and C. Chihta, "The transient optical Kerr effect of simple liquids studied with an ultrashort laser with variable pulsewidth," IEEE J. Sel. Top. Quantum Electron. **2**, 756–768 (1996).
40. Y. Sato, R. Morita, and M. Yamashita, "Study on ultrafast dynamic behaviors of different nonlinear refractive index components in CS_2 using a femtosecond interferometer," Jpn. J. Appl. Phys. **36**, 2109–2115 (1997).
41. M. Reichert, P. Zhao, J. M. Reed, T. R. Ensley, D. J. Hagan, and E. W. Van Stryland, "Beam deflection measurement of bound-electronic and rotational nonlinear refraction in molecular gases: erratum," Opt. Express **24**, 19122 (2016).
42. P. Zhao, M. Reichert, D. J. Hagan, and E. W. Van Stryland, "Dispersion of nondegenerate nonlinear refraction in semiconductors," Opt. Express **24**, 24907–24920 (2016).
43. S. Benis, D. J. Hagan, and E. W. Van Stryland, "Cross-propagating beam-deflection measurements of third-order nonlinear optical susceptibility," in *SPIE LASE* (SPIE, 2017), p. 6.
44. Y. Li, D. Y. Chen, L. Yang, and R. R. Alfano, "Ultrafast all-optical deflection based on an induced area modulation in nonlinear materials," Opt. Lett. **16**, 438–440 (1991).
45. A. Dogariu, T. Xia, D. J. Hagan, A. A. Said, E. W. Van Stryland, and N. Bloembergen, "Purely refractive transient energy transfer by stimulated Rayleigh-wing scattering," J. Opt. Soc. Am. B **14**, 796–803 (1997).
46. R. A. Negres, J. M. Hales, A. Kobyakov, D. J. Hagan, and E. W. Van Stryland, "Experiment and analysis of two-photon absorption spectroscopy using a white-light continuum probe," IEEE J. Quantum Electron. **38**, 1205–1216 (2002).
47. K. J. Miller, "Calculation of the molecular polarizability tensor," J. Am. Chem. Soc. **112**, 8543–8551 (1990).
48. J. Applequist, J. R. Carl, and K.-K. Fung, "Atom dipole interaction model for molecular polarizability. Application to polyatomic molecules and determination of atom polarizabilities," J. Am. Chem. Soc. **94**, 2952–2960 (1972).
49. G. R. Alms, A. K. Burnham, and W. H. Flygare, "Measurement of the dispersion in polarizability anisotropies," J. Chem. Phys. **63**, 3321–3326 (1975).
50. R. Bramley, C. G. Le Fevre, R. J. W. Le Fevre, and B. P. Rao, "232. Molecular polarisability. The anisotropy of the C=C bond," J. Chem. Soc. (Resumed) **0**, 1183–1188 (1959).
51. S. Constantine, J. A. Gardecki, Y. Zhou, L. D. Ziegler, X. Ji, and B. Space, "A novel technique for the measurement of polarization-specific ultrafast Raman responses," J. Phys. Chem. A **105**, 9851–9858 (2001).
52. C. J. Fecko, J. D. Eaves, and A. Tokmakoff, "Isotropic and anisotropic Raman scattering from molecular liquids measured by spatially masked optical Kerr effect spectroscopy," J. Phys. Chem. **117**, 1139–1154 (2002).
53. Q.-H. Xu, Y.-Z. Ma, and G. R. Fleming, "Heterodyne detected transient grating spectroscopy in resonant and non-resonant systems using a simplified diffractive optics method," Chem. Phys. Lett. **338**, 254–262 (2001).
54. M. Thalhammer and A. Penzkofer, "Measurement of third-order nonlinear susceptibilities by non-phase matched third-harmonic generation," Appl. Phys. B **32**, 137–143 (1983).
55. B. F. Levine and C. G. Bethea, "Second and third order hyperpolarizabilities of organic molecules," J. Chem. Phys. **63**, 2666–2682 (1975).
56. R. J. Bartlett and G. D. Purvis, "Molecular hyperpolarizabilities. I. Theoretical calculations including correlation," Phys. Rev. A **20**, 1313–1322 (1979).
57. D. P. Shelton and J. E. Rice, "Measurements and calculations of the hyperpolarizabilities of atoms and small molecules in the gas phase," Chem. Rev. **94**, 3–29 (1994).
58. A. Willetts, J. E. Rice, D. M. Burland, and D. P. Shelton, "Problems in the comparison of theoretical and experimental hyperpolarizabilities," J. Chem. Phys. **97**, 7590–7599 (1992).
59. A. Tokmakoff, M. J. Lang, D. S. Larsen, G. R. Fleming, V. Chernyak, and S. Mukamel, "Two-dimensional Raman spectroscopy of vibrational interactions in liquids," Phys. Rev. Lett. **79**, 2702–2705 (1997).
60. F. Kajzar and J. Messier, "Third-harmonic generation in liquids," Phys. Rev. A **32**, 2352–2363 (1985).
61. A. K. Burnham and T. D. Gierke, "A comparison of effective polarizabilities from electro-optical experiments using microscopic and macroscopic theories of the local electric field," J. Chem. Phys. **73**, 4822–4831 (1980).
62. K. Kiyohara, K. Kamada, and K. Ohta, "Orientational and collision-induced contribution to third-order nonlinear optical response of liquid CS_2," J. Chem. Phys. **112**, 6338–6348 (2000).
63. T. R. Ensley, H. Hu, M. Reichert, M. R. Ferdinandus, D. Peceli, J. M. Hales, J. W. Perry, Z. A. Li, S.-H. Jang, A. K. Y. Jen, S. R. Marder, D. J. Hagan, and E. W. Van Stryland, "Quasi-three-level model applied to measured spectra of nonlinear absorption and refraction in organic molecules," J. Opt. Soc. Am. B **33**, 780–796 (2016).
64. M. R. Ferdinandus, M. Reichert, T. R. Ensley, H. Hu, D. A. Fishman, S. Webster, D. J. Hagan, and E. W. Van Stryland, "Dual-arm Z-scan technique to extract dilute solute nonlinearities from solution measurements," Opt. Mater. Express **2**, 1776–1790 (2012).
65. Z. A. Li, T. R. Ensley, H. Hu, Y. Zhang, S.-H. Jang, S. R. Marder, D. J. Hagan, E. W. Van Stryland, and A. K. Y. Jen, "Conjugated polycyanines: a new class of materials with large third-order optical nonlinearities," Adv. Opt. Mater. **3**, 900–906 (2015).
66. Z. A. Li, P. Zhao, S. Tofighi, R. Sharma, T. R. Ensley, S.-H. Jang, D. J. Hagan, E. W. Van Stryland, and A. K.-Y. Jen, "Zwitterionic cyanine-cyanine salt: structure and optical properties," J. Phys. Chem. C **120**, 15378–15384 (2016).
67. H. Hu, T. R. Ensley, M. Reichert, M. R. Ferdinandus, D. Peceli, O. V. Przhonska, S. R. Marder, A. K. Y. Jen, J. M. Hales, J. W. Perry, D. J. Hagan, and E. W. Van Stryland, "Optimization of the electronic third-order nonlinearity of cyanine-like molecules for all optical switching," Proc. SPIE **8983**, 898303 (2014).
68. J. M. Hales, D. J. Hagan, E. W. Van Stryland, K. J. Schafer, A. R. Morales, K. D. Belfield, P. Pacher, O. Kwon, E. Zojer, and J. L. Bredas, "Resonant enhancement of two-photon absorption in substituted fluorene molecules," J. Chem. Phys. **121**, 3152–3160 (2004).
69. S. Shahin, K. Kieu, J. M. Hales, H. Kim, Y. A. Getmanenko, Y. Zhang, J. W. Perry, S. R. Marder, R. A. Norwood, and N. Peyghambarian, "Third-order nonlinear optical characterization of organic chromophores using liquid-core optical fibers," J. Opt. Soc. Am. B **31**, 2455–2459 (2014).